ISSN 2616-5767 Vol.5, Issue 1: 34-40, DOI: 10.25236/AJETS.2022.050107

Numerical Simulation of Pressure Distribution Changes in Porous Rocks under the Action of High Pressure Fluid

Jiajing Li[a*], Zhe Liu[b], Chao Wang[c], Yingjie Dong[d], Fengying Guo[e]

School of Petroleum Engineering, Guangdong University of Petrochemical Technology, Maoming 525000, Guangdong, China
[a]lijiajing@gdupt.edu.cn, [b]liuzhe@gdupt.edu.cn, [c]wangttyingjie@163.com, [d]412864418@qq.com, [e]1132844763@qq.com
**Corresponding author*

Abstract: *The rock medium has the characteristics of heterogeneity, opacity and porosity. Fluid injection (such as hydraulic fracturing technology) can make the tight rock mass form a gas permeability enhancement zone near the borehole, which is conducive to unconventional natural gas extraction. Compared with experimental research, numerical simulation research has lower cost and higher efficiency, and has become an important method for research on fluid interaction and pore pressure. Based on this, this article mainly conducts a numerical simulation study on the changes in the internal pressure distribution of porous rocks under the action of high-pressure fluid (HPF). This article outlines the mechanism of quasi-static HPF fracturing coal and rock, and describes the classification of tensile fracture and shear fracture. In this paper, a numerical simulation method is used to construct a model of a porous rock sample, and a test of the internal pressure of the porous rock under the action of a HPF is carried out on the rock simulation sample. The experiment shows that when the intermediate principal stress σ2 is 20 MPa, the peak pressure of fluid* H_2O *is 12.5 MPa; when σ 2 is 25 MPa, the peak fluid pressure of* H_2O *is 12 MPa. This shows that the intermediate principal stress (or horizontal stress difference) is negatively related to the maximum fluid pressure.*

Keywords: *Pore Rock, High Pressure Fluid, Numerical Simulation, Internal Pressure of Rock*

1. Introduction

A complex pore structure is formed inside the natural rock, which will affect the failure characteristics and mechanical properties of the rock mass, making the rock mass more complex than homogeneous materials, showing nonlinearity, discontinuity and anisotropy [1-2] . Fluid action and the pore structure inside the rock have a great influence on its physical and mechanical properties, energy storage efficiency and permeability characteristics under environmental factors [3-4]. In addition to the main components of rock blocks, rocks also contain various irregular and cross-scale pore defects. These structural features have a significant impact on the mechanical properties and failure modes of the rock [5-6]. The pore deformation caused by fluid flow will eventually cause the deformation of the rock. It is of great significance to explore the changes in the internal pressure distribution of porous rocks under the action of HPF.

Regarding the study of pore pressure, many scholars have conducted multi-angle discussions. For example, Zhou ZH studied the influence of excess pore pressure on low-slope river debris flow and long runoff [7]; Wei C studied the influence of pressure and fluid on dolomite the influence of pore geometry and elasticity [8]; Wang HT considers the influence of pore water pressure, therefore, predicts the roof support pressure of layered soil shallow tunnels [9]. Therefore, this article focuses on the internal pressure distribution changes of porous rocks under the action of HPF, which is of great significance to underground engineering, mining engineering, foundation engineering, rock crushing and blasting engineering, etc.

The purpose of this paper is to study the numerical simulation of the pressure distribution changes in porous rocks under the action of HPF. This paper firstly takes coal and rock as an example, introduces the mechanism of quasi-static HPF fracturing coal and rock, and explains the stress changes in tensile fracture and shear fracture in all directions. This paper uses RFPA3D-CT software to

ISSN 2616-5767 Vol.5, Issue 1: 34-40, DOI: 10.25236/AJETS.2022.050107

construct a simulation model of a rock sample, and conducts a triaxial compression numerical simulation test of the pressure distribution change in a porous rock under the action of a HPF.

2. Analysis of Internal Pressure of Porous Rock under the Action of HPF

2.1 Quasi-Static HPF Fracturing Coal

Coal rock is a typical porous rock mass, which contains face cleats parallel to the bedding direction and good continuity, and also contains end cleats perpendicular to the bedding direction and poor continuity [10-11]. A large number of natural fractures in coal seams are conducive to the production of complex fracture networks, but at the same time it also increases the uncertainty of fracture propagation.

Injecting fluid into the coal seam through boreholes and gradually increasing the fluid injection pressure to crack the coal seam [12]. This process takes a long time and can be regarded as a quasi-static high-pressure process. According to the stress state of the borehole wall, the fracture of the quasi-static high-pressure fractured coal seam can be divided into tensile fracture and shear fracture.

(1) Tensile fracture

Assuming that there is a circular borehole in the coal seam, the coal seam is affected by the ground stress, the vertical stress, the horizontal maximum and the minimum ground stress. As the fluid is injected, the fluid pressure continues to increase. When the stress on the borehole wall exceeds the tensile strength of the coal rock, the coal rock ruptures and causes cracks. This is the most commonly used tensile rupture criterion in many fields such as coal mines and oil and gas. Considering the fluid pressure when σ =0, the tangential stress of the borehole wall reaches the minimum value. The calculation method is as shown in formula (1):

$$\sigma_\theta = 3\sigma_{\mathrm{h}} - \sigma_H - P \tag{1}$$

θ represents the angle between a certain position in the rock mass and the maximum principal stress (the angle rotated in the counterclockwise direction), σ_H represents the maximum horizontal principal stress, and σ_{h} represents the minimum horizontal principal stress. When fluid fracturing a coal seam, as the fluid pressure P continues to increase, σ_θ gradually decreases and becomes a tensile stress. When σ_θ exceeds the tensile strength of the coal rock, the coal rock ruptures and causes cracks. The tensile rupture criterion can be expressed by formula (2):

$$P \geq 3\sigma_\theta - \sigma_H + T \tag{2}$$

In the formula, T represents the tensile strength of coal.

(2) Shear rupture

The coal seam structure conditions are complex, and the tensile fracture criterion only considers the influence of σ_θ, while ignoring the influence of σ_{r} (tangential stress, r=radius of the circular borehole) and σ_{z}. Changes in the principal stresses in the three directions may cause shear failure of the borehole wall. Therefore, in this paper, the Mohr-Coulomb criterion is used to analyze the shear fracture in the process of fluid fracturing coal and rock. The expressions of the Mohr-Coulomb criterion are shown in (3), (4), (5), (6):

$$\tau = \mathrm{c} + \sigma_n \tan\varphi \tag{3}$$

$$\tau = \frac{\sigma_1 - \sigma_3}{2}\sin 2\alpha \tag{4}$$

$$\sigma_{\mathrm{n}} = \frac{\sigma_1 + \sigma_3}{2} + \frac{\sigma_1 - \sigma_3}{2}con2\alpha \tag{5}$$

ISSN 2616-5767 Vol.5, Issue 1: 34-40, DOI: 10.25236/AJETS.2022.050107

$$\alpha = 45^{\circ} + \frac{\varphi}{2} \tag{6}$$

In the formula, τ represents the shear stress of the fracture surface, σ_n represents the normal stress of the fracture surface, α represents the angle between the reverse direction of the fracture surface and the maximum principal stress, φ represents the internal friction angle of the coal and rock, and c represents the rock cohesion.

If there is only normal stress in the rock force process, and the shear stress is excluded, the principal stress in the three directions of the borehole wall can be calculated under the action of fluid pressure, as shown in formulas (7), (8), (9), respectively Shown:

$$\sigma_r = P \tag{7}$$

$$\sigma_\theta = \sigma_H + \sigma_h - 2(\sigma_H - \sigma_h)con2\theta - P \tag{8}$$

$$\sigma_z = \sigma_v - v[2(\sigma_H + \sigma_h)con2\theta] - P \tag{9}$$

It can be seen from the above formula that in the process of injecting fluid into the coal seam, as the fluid pressure increases, σ_r of the borehole wall continues to increase, and σ_θ and σ_z continue to decrease.

2.2 Porosity of Porous Coal

The index to measure the number of pores in a coal body is porosity, which refers to the ratio of the sum of the volume of fine pores and cracks in the coal body to the total volume of the coal body. It is also called porosity and is usually expressed as a percentage. The calculation method is as shown in formula (10) Show:

$$K\ (\%) = \frac{V_p - V_t}{V_p} \times 100\% \tag{10}$$

In the formula, V_p represents the total volume of the rock itself and its pores, mL; V_t represents the actual volume of the rock, excluding the volume of pores, mL.

The porosity of the rock is closely related to the grade of the rock, the composition of the microscopic rock, and the mineral content in the rock. In addition, the degree of metamorphism of coal and rock also affects the porosity of the rock mass. On the whole, the porosity of rocks with moderate metamorphism is the smallest. The porosity of different rocks is very different, even for similar rocks, the porosity is also very different. According to the diameter of the pores, rock pores can be divided into the following categories: pores with a diameter less than 10nm are called micropores; pores with a diameter between 100nm and 1000nm are called small pores; pores with a diameter greater than 1000nm are called macropores. The porosity of the same type of rock can have a considerable range of fluctuations.

3. Numerical Simulation Design

3.1 Numerical Simulation System

In the summary of this experiment, the RFPA3D-CT software (Realistic Failure Process Analysis) was used to construct the model and carry out the numerical simulation experiment. The model constructed by this software can take into account the discontinuity and non-uniformity of the rock, and better simulate the whole process of the change of the internal pressure distribution of the porous rock under the action of the HPF.

3.2 Numerical Model and Scheme

First, determine the simulated sample material that can form porous rock in the system, add

ISSN 2616-5767 Vol.5, Issue 1: 34-40, DOI: 10.25236/AJETS.2022.050107

corresponding joints on this basis to form a complete porous rock sample model, and finally get macro test results similar to the real test by adjusting the parameters. And then conduct follow-up analysis and research.

(1) Simulation model

The size of the model is width×height=50mm×100mm, joints are added between each layer of the rock sample, and the rock layer is inclined at 45°.

(2) Simulation plan

The loading rate of 0.05m/s in this paper is far less than 0.2m/s, so the loading rate set in this paper can ensure that the model sample is statically loaded.

The interruption condition in the numerical simulation test is: when the axial stress of the sample is loaded to the peak and drops to 70% of the peak strength, the program stops the calculation and the numerical simulation test is completed.

3.3 Experimental Protocol

In this study, numerical simulation experiments on the influence of the interaction of pressurized fluids with different viscosities and intermediate principal stresses on the deformation, strength characteristics and crack growth behavior of rock samples under triaxial stress conditions were carried out. The rock samples were subjected to numerical simulation experiments in such a way that the bedding plane was perpendicular to the X direction, the face cleats were perpendicular to the Z direction, and the end cleats were perpendicular to the Y direction. The specific values of the rock sample strength under full stress conditions are shown in Table 1:

Table 1: Strength of simulated porous rock samples under triaxial stress conditions (unit: MPa)

X(σ3)	Z(σ2)	Y(σ1)
15	15	50
15	20	60
15	30	65
15	40	70
15	50	75

In addition, the study used H_2O, N_2, and CO_2 as HPFs.

4. Numerical Simulation Experiment Results

4.1 Deformation and Fracture Characteristics of Rock Specimens under the Action of Pressurized Fluid

The experiment shows that the relationship between the peak fluid pressure and the intermediate principal stress σ2 and the horizontal stress difference (σ2-σ3) is shown in Table 2: When σ2 is 20MPa, the peak fluid pressure of N_2 is 12MPa; when σ2 is 25MPa, the relationship between N_2 fluid the peak pressure is 11MPa. When σ2 is 20MPa, the peak pressure of fluid H_2O is 12.5MPa; when σ2 is 25MPa, the peak pressure of fluid H_2O is 12MPa.

Table 2: The relationship between the peak fluid pressure and the intermediate principal stress σ2 (unit: MPa)

σ2/MPa	N_2 (Nitrogen)	H_2O (Gaseous water)	CO_2 (carbon dioxide)
20	12	12.5	11.5
25	11	12	11
30	10	11.8	10.5
35	9.8	11.5	10.2
40	9.5	11.4	9.5
45	9.2	11	9.4
50	9	10	9.2

ISSN 2616-5767 Vol.5, Issue 1: 34-40, DOI: 10.25236/AJETS.2022.050107

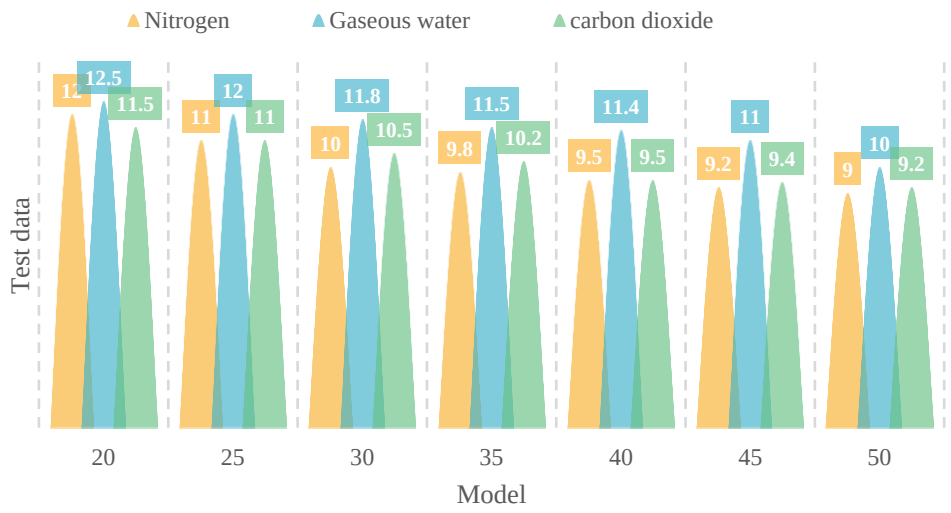

Figure 1: The relationship between the peak fluid pressure and the intermediate principal stress σ2 (unit: MPa)

It can be seen from Figure 1 that with the increase of the intermediate principal stress σ2 (or the horizontal stress difference), the maximum fluid pressure when the rock sample fails is reduced, and the maximum fluid pressure during pressurized water injection is stronger than that of carbon dioxide and nitrogen. In the numerical simulation experiment, the greater the intermediate principal stress, the stronger the compression effect on the cleat, and correspondingly, the expansion effect of the pore pressure on its deformation is weakened.

When a large amount of fluid pressure accumulates in the bedding and the cracks distributed along the bedding plane, the offsetting effect on the minimum principal stress is enhanced. It can be seen that as the pore pressure increases, the effective stress effect of the rock sample in the direction of the minimum principal stress increases, which is equivalent to the minimum principal stress being unloaded. The larger the σ2, the more significant the unloading effect. Eventually, the rock sample was destabilized and damaged. Therefore, the intermediate principal stress (or horizontal stress difference) is negatively related to the maximum fluid pressure.

4.2 Influence of Different HPF Injection on the Pressure Distribution inside the Rock

In the process of pressurized fluid injection, the change values of the principal stress in each direction of the rock sample before failure are shown in Table 3: Among them, σ3=15MPa, σ1=50MPa.

Table 3: Changes of principal stress in each direction of the rock sample before failure during pressurized fluid injection

Pressurized fluid	σ2/MPa	Δε3/%	Δε1/%	Δε2/%
Nitrogen	20	-0.140	0.209	-0.066
	30	-0.143	0.130	0.020
	40	-0.437	0.093	0.083
	50	-0.850	0.059	0.541
Gaseous water	20	-0.029	0.157	-0.018
	30	-0.043	0.089	0.021
	40	-0.194	0.071	0.063
	50	-0.150	0.044	0.107
carbon dioxide	20	-0.301	0.183	-0.129
	30	-0.471	0.129	-0.063
	40	-0.347	0.120	0.101
	50	-0.662	0.059	0.294

ISSN 2616-5767 Vol.5, Issue 1: 34-40, DOI: 10.25236/AJETS.2022.050107

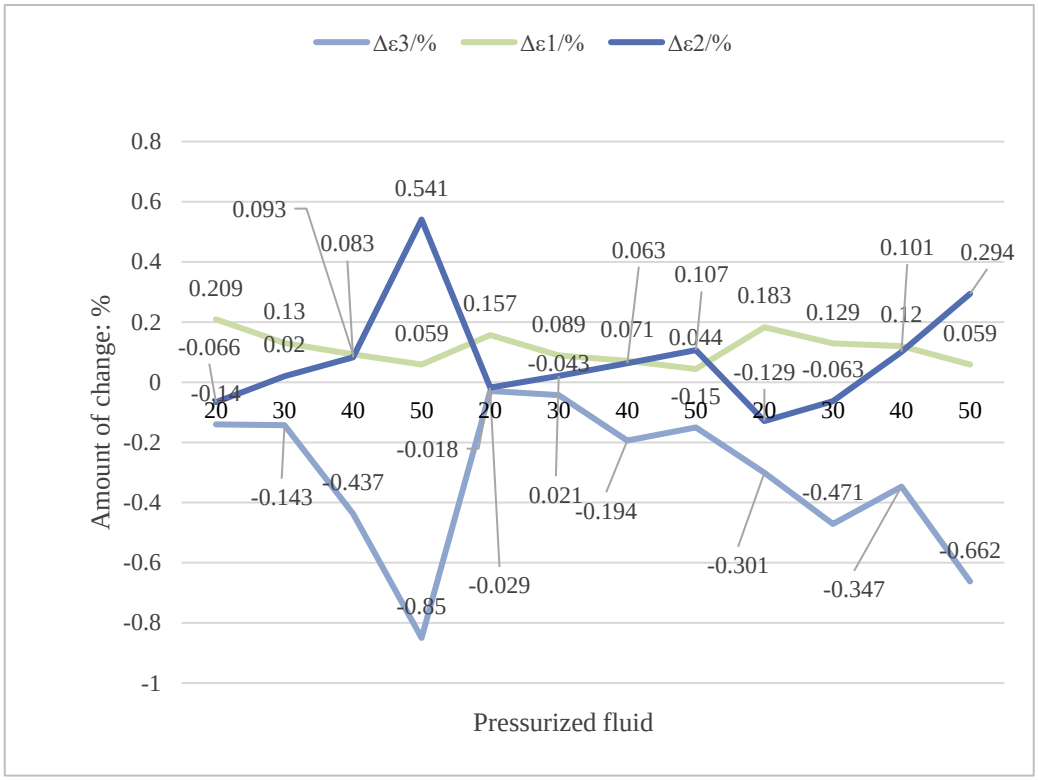

Figure 2: Changes of principal stress in each direction of the rock sample before failure during pressurized fluid injection

It can be seen from Figure 2 that during the process of fluid pressurization, the deformation of the rock simulation specimen in the direction of the maximum principal stress is always in a compressed state, and the deformation Δε3 in the direction of the minimum principal stress is greater than the deformation Δε2 in the direction of the intermediate principal stress. Even when the intermediate principal stress is at a relatively low level, the rock simulation test is also in a state of expansion in the σ2 direction. This indicates that the offset effect of pore pressure on σ1 (effective stress effect) under the action of liquid pressure is weaker than the offset effect of pore pressure on σ2 and σ3, and the offset effect of pore pressure on σ2 is weaker than that of pore pressure on σ3. Therefore, as the fluid pressure and pore pressure in the rock simulation sample increase, the effective stress effects in the main stress directions inside the rock are from strong to weak: minimum principal stress direction>middle principal stress direction>maximum principal stress direction.

5. Conclusions

The rock has a unique bedding structure and cleat structure, and pore pressure and HPF have anisotropic characteristics for its action. Using numerical simulation methods, it is possible to observe the process of crack propagation and penetration on the surface and internal of the rock sample. Numerical simulation results help to reveal the influence law of rock macroscopic failure under the action of HPF and pores, and solve the problem that the internal structure of the rock and the failure process are difficult to observe. In this paper, numerical simulation method is used to test the internal pressure change of porous rock under the action of HPF on the rock sample. The effective stress effect in the principal stress direction from strong to weak is: the minimum principal stress direction>the intermediate principal stress direction>the maximum principal stress direction.

Acknowledgements

This work was supported by The National Natural Science Foundation of China (41602154) and Projects of Talents Recruitment of GDUPT (2018rc01)

ISSN 2616-5767 Vol.5, Issue 1: 34-40, DOI: 10.25236/AJETS.2022.050107

References

[1] Neupane B, Panthi K K , Vereide K . Effect of Power Plant Operation on Pore Pressure in Jointed Rock Mass of an Unlined Hydropower Tunnel: An Experimental Study[J]. Rock Mechanics and Rock Engineering, 2020, 53(7):3073-3092.

[2] Dakhelpour-Ghoveifel J , Shahverdi H . Prediction of gas-oil capillary pressure of carbonate rock using pore network modeling[J]. Journal of Petroleum Science and Engineering, 2020, 195(2):107861.

[3] Lei T , Yin X , Zong Z . Pore pressure prediction in orthotropic medium based on rock physics modeling of shale gas[J]. Journal of Natural Gas Science and Engineering, 2019, 74(11):103091.

[4] Braun P , Ghabezloo S , Delage P , et al. Theoretical Analysis of Pore Pressure Diffusion in Some Basic Rock Mechanics Experiments[J]. Rock Mechanics & Rock Engineering, 2018, 51(5):1-18.

[5] Garing C , Chalendar J D , Voltolini M , et al. Pore-scale capillary pressure analysis using multi-scale X-ray micromotography[J]. Advances in Water Resources, 2017, 104(jun.):223-241.

[6] De Carvalho T P , Morvan H P , Hargreaves D M , et al. Pore-Scale Numerical Investigation of Pressure Drop Behaviour Across Open-Cell Metal Foams[J]. Transport in Porous Media, 2017, 117(3):1-26.

[7] Zhou Z H , Ren Z , Wang K , et al. Effect of excess pore pressure on the long runout of debris flows over low gradient channels: A case study of the Dongyuege debris flow in Nu River, China[J]. Geomorphology, 2018, 308(MAY1):40-53.

[8] Wei C , Carcione J M , Picotti S , et al. Effect of pressure and fluid on pore geometry and anelasticity of dolomites[J]. Rheologica Acta, 2020, 59(11).

[9] Wang H T , Li X J , Liu P , et al. Prediction of roof supporting pressure for shallow tunnels in layered soils incorporating the effect of pore water pressure[J]. PLoS ONE, 2019, 14(6):e0217351.

[10] Song I H , Bae B S , Ha J H , et al. Effect of Hydraulic Pressure on Alumina Coating on Pore Characteristics of Flat-Sheet Ceramic Membrane[J]. Ceramics International, 2017, 43(13):10502-10507.

[11] Yi M , Cheng Y , Wang Z , et al. Effect of particle size and adsorption equilibrium time on pore structure characterization in low pressure N2 adsorption of coal: An experimental study[J]. Advanced Powder Technology, 2020, 31(10):4275-4281.

[12] Aliha M , Bahmani A . Rock Fracture Toughness Study Under Mixed Mode I/III Loading[J]. Rock Mechanics & Rock Engineering, 2017, 50(7):1-13.